Journal of Thermal Stresses
Publication details, including instructions for authors and subscription information:
http://www.informaworld.com/smpp/title~content=t713723680

Estimation of Heat Flux and Thermal Stresses in Functionally Graded Hollow Circular Cylinders

Win-Jin Chang[a]; Haw-Long Lee[a]; Yu-Ching Yang[a]
[a] Clean Energy Center, Department of Mechanical Engineering, Kun Shan University, Taiwan, Republic of China

Online publication date: 23 May 2011

To cite this Article Chang, Win-Jin , Lee, Haw-Long and Yang, Yu-Ching(2011) 'Estimation of Heat Flux and Thermal Stresses in Functionally Graded Hollow Circular Cylinders', Journal of Thermal Stresses, 34: 7, 740 — 755
To link to this Article: DOI: 10.1080/01495739.2010.550835
URL: http://dx.doi.org/10.1080/01495739.2010.550835

Journal of Thermal Stresses, 34: 740–755, 2011

ISSN: 0149-5739 print/1521-074X online
DOI: 10.1080/01495739.2010.550835

ESTIMATION OF HEAT FLUX AND THERMAL STRESSES IN FUNCTIONALLY GRADED HOLLOW CIRCULAR CYLINDERS

Win-Jin Chang, Haw-Long Lee, and Yu-Ching Yang
Clean Energy Center, Department of Mechanical Engineering, Kun Shan University, Taiwan, Republic of China

In this study, an inverse algorithm based on the conjugate gradient method and the discrepancy principle is applied to estimate the unknown time-dependent heat flux at the inner surface of a functionally graded hollow circular cylinder from the knowledge of temperature measurements taken within the cylinder. Subsequently, the distributions of temperature and thermal stresses in the cylinder can be determined as well. It is assumed that no prior information is available on the functional form of the unknown heat flux; hence the procedure is classified as the function estimation in inverse calculation. The temperature data obtained from the direct problem are used to simulate the temperature measurements, and the effect of the errors in these measurements upon the precision of the estimated results is also considered. Results show that an excellent estimation on the time-dependent heat flux, temperature distributions, and thermal stresses can be obtained for the test case considered in this study.

Keywords: Conjugate gradient method; Functionally graded cylinder; Heat flux; Inverse problem

INTRODUCTION

Quantitative studies of heat transfer processes occurring in many industrial applications often require accurate knowledge of boundary conditions, such as heat flux, or thermophysical properties of the materials involved. These important quantities were conventionally obtained by expensive experimental methods which normally involve delicate and sophisticated equipments. In recent years, however, the studies of inverse heat conduction problem (IHCP) have offered convenient alternatives, which largely scale down experimental work, to obtain accurate thermophysical quantities such as heat sources, material's thermal properties, and boundary temperature or heat flux distributions, in many heat conduction problems [1–4]. In these cases, the direct heat conduction problems are concerned with the determination of temperature at interior points of a region when the initial and boundary conditions, heat generation, and material properties are specified, whereas, the inverse heat conduction problem (IHCP) involves the determination of the surface conditions, energy generation, thermophysical properties, etc., from the

Received 7 September 2010; accepted 5 November 2010.
Address correspondence to Yu-Ching Yang, Clean Energy Center, Department of Mechanical Engineering, Kun Shan University, Yung-Kang City, Tainan 710-03, Taiwan, Republic of China. E-mail: ycyang@mail.ksu.edu.tw

knowledge of temperature measurements taken within the body. To date, a variety of analytical and numerical techniques have been developed for the solution of the inverse heat conduction problems, for example, the conjugate gradient method (CGM) [5–8], the Tikhonov regularization method [9], and the genetic algorithm [10], etc.

Functionally graded materials (FGMs) have been proposed as a solution for the aerospace industry where high-temperature, light-weight structures are required to meet the challenges faced by future high-speed air vehicles. These novel materials have excellent thermo-mechanical properties to withstand high temperature and also have extensive applications to important structures, such as aerospace, nuclear reactors, pressure vessels and pipes, chemical plants, etc. [11–13]. On the other hand, current thermal protection systems are parasitic in that they carry no significant structural load and require time-consuming inspection and replacement.

FGMs that continuously transition from ceramic to metallic materials would avoid the mismatch of the coefficient of thermal expansion found in dissimilar materials. Hence, the inverse heat conduction analysis of FGMs is an important and challenging problem. The inverse heat conduction analysis of isotropic materials has been studied by many authors; however, to the best of authors' knowledge, there are few researches on the inverse heat conduction of FGMs [14].

The focus of the present study is to develop an inverse analysis for estimating the unknown time-dependent heat flux at the inner surface of a functionally graded hollow circular cylinder from the knowledge of temperature measurements taken within the cylinder. Subsequently, the distributions of temperature and thermal stresses in the cylinder can be determined as well. An analysis of this kind poses significant implications on several industrial applications such as aerospace, nuclear reactors, pressure vessels and pipes, chemical plants, etc. Here, we present the conjugate gradient method and the discrepancy principle [15] to estimate the unknown time-dependent heat flux by using the simulated temperature measurements. The conjugate gradient method with an adjoint equation, also called Alifanov's iterative regularization method, belongs to a class of iterative regularization techniques, which mean the regularization procedure is performed during the iterative processes, thus the determination of optimal regularization conditions is not needed. No prior information is used in the functional form of the heat flux variation with time. On the other hand, the discrepancy principle is used to terminate the iteration process in the conjugate gradient method.

ANALYSIS

Direct Problem

To illustrate the methodology for developing expressions for the use in determining the unknown time-dependent heat flux at the inner surface of a functionally graded hollow circular cylinder, a FGM cylinder with inner radius r_1, outer radius r_2, and infinite length, as shown in Figure 1, is considered herein. Assume the cylinder is initially at zero temperature, the outer surrounding temperature $T_\infty = 0$, and for time $t > 0$, the cylinder is suddenly subjected to a heat flux $q(t)$ at its inner boundary surface $r = r_1$. The convection heat transfer

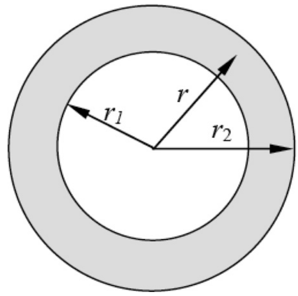

Figure 1 Geometry and coordinate system.

coefficient at the outer surface is h. Then the dimensionless governing equations and the associated boundary and initial conditions for the system can be written as [11]:

$$\frac{\partial^2 T^*(r^*, t^*)}{\partial r^{*2}} + \left[\frac{1}{r^*} + \frac{\mathrm{d}k^*(r^*)/\mathrm{d}r^*}{k^*(r^*)}\right]\frac{\partial T^*(r^*, t^*)}{\partial r^*} = \frac{1}{\alpha^*(r^*)}\frac{\partial T^*(r^*, t^*)}{\partial t^*} \quad (1)$$

$$-k^*(r^*)\frac{\partial T^*(r^*, t^*)}{\partial r^*} = q^*(t^*), \quad \text{at } r^* = r_1^* \quad (2)$$

$$k^*(r^*)\frac{\partial T^*(r^*, t^*)}{\partial r^*} + Bis \cdot T^*(r^*, t^*) = 0, \quad \text{at } r^* = r_2^* \quad (3)$$

$$T^*(r^*, t^*) = 0, \quad \text{for } t^* = 0 \quad (4)$$

The dimensionless variables used in the above formulation are defined as follows:

$$\begin{aligned} &r^* = r/r_1, \quad r_1^* = r_1/r_1, \quad r_2^* = r_2/r_1, \quad t^* = \alpha_0 t/r_1^2, \quad T^* = T/T_0, \\ &k^* = k/k_0, \quad \alpha^* = \alpha/\alpha_0, \quad Bis = hr_1/k_0, \quad q^* = r_1 q/k_0 T_0 \end{aligned} \quad (5)$$

where T_0 is a reference temperature; k_0, and α_0 are reference values of thermal conductivity and thermal diffusivity, respectively. Moreover, in this study, we assume the thermal conductivity k and thermal diffusivity α change smoothly and continuously through the thickness of the FGM hollow circular cylinder. The direct problem considered here is concerned with the determination of the medium temperature when the heat flux $q^*(t^*)$, thermophysical properties of the cylinders, and initial and boundary conditions are known. A hybrid numerical method of Laplace transformation and finite difference used in our previous work can be applied to solve the direct problem [16].

Inverse Problem

For the inverse problem, the function $q^*(t^*)$ is regarded as being unknown, while everything else in Eqs. (1)–(4) is known. In addition, temperature readings taken at $r = r_m$ are considered available. The objective of the inverse analysis is to predict the unknown time-dependent heat flux, $q^*(t^*)$, merely from the knowledge of these temperature readings. Let the measured temperature at the measurement position $r = r_m$ and time t be denoted by $Y(r_m, t)$. Then this inverse problem can be stated as follows: by utilizing the above mentioned measured temperature data $Y(r_m, t)$, the unknown $q^*(t^*)$ is to be estimated over the specified time domain.

The solution of the present inverse problem is to be obtained in such a way that the following functional is minimized:

$$J[q^*(t^*)] = \int_{t^*=0}^{t_f^*} [T^*(r_m^*, t^*) - Y^*(r_m^*, t^*)]^2 \mathrm{d}t^* \tag{6}$$

where $Y^*(r_m^*, t^*) = Y(r_m, t)/T_0$, and $T^*(r_m^*, t^*)$ is the estimated (or computed) temperature at the measurement location $r^* = r_m^*$. In this study, $T^*(r_m^*, t^*)$ are determined from the solution of the direct problem given previously by using an estimated $q^{*K}(t^*)$ for the exact $q^*(t^*)$, here $q^{*K}(t^*)$ denotes the estimated quantities at the Kth iteration. t_f^* is the final time of the measurement. In addition, in order to develop expressions for the determination of the unknown $q^*(t^*)$, a "sensitivity problem" and an "adjoint problem" are constructed as described next.

Sensitivity Problem and Search Step Size

The sensitivity problem is obtained from the original direct problem defined by Eqs. (1)–(4) in the following manner: It is assumed that when $q^*(t^*)$ undergoes a variation $\Delta q^*(t^*)$, $T^*(r^*, t^*)$ is perturbed by $T^*(r^*, t^*) + \Delta T^*(r^*, t^*)$. Then replacing in the direct problem q^* by $q^* + \Delta q^*$ and T^* by $T^* + \Delta T^*$, subtracting from the resulting expressions the direct problem, and neglecting the second-order terms, the following sensitivity problem for the sensitivity function ΔT^* can be obtained.

$$\frac{\partial^2 \Delta T^*}{\partial r^{*2}} + \left[\frac{1}{r^*} + \frac{\mathrm{d}k^*(r^*)/\mathrm{d}r^*}{k^*(r^*)}\right] \frac{\partial \Delta T^*}{\partial r^*} = \frac{1}{\alpha^*(r^*)} \frac{\partial \Delta T^*}{\partial t^*}, \tag{7}$$

$$-k^*(r^*) \frac{\partial \Delta T^*}{\partial r^*} = \Delta q^*(t^*), \quad \text{at } r^* = r_1^*, \tag{8}$$

$$k^*(r^*) \frac{\partial \Delta T^*(r^*, t^*)}{\partial r^*} + Bis \cdot \Delta T^*(r^*, t^*) = 0, \quad \text{at } r^* = r_2^*, \tag{9}$$

$$\Delta T^*(r^*, t^*) = 0, \quad \text{for } t^* = 0, \tag{10}$$

The sensitivity problem of Eqs. (7)–(10) can be solved by the same method as the direct problem of Eqs. (1)–(4).

Adjoint Problem and Gradient Equation

To formulate the adjoint problem, Eqs. (1) is multiplied by the Lagrange multiplier (or adjoint function) $\lambda(r^*, t^*)$, and the resulting expressions are integrated over the time and correspondent space domains. Then the results are added to the right hand side of Eq. (6) to yield the following expression for the functional $J[q^*(t^*)]$:

$$J[q^*(t^*)] = \int_{t^*=0}^{t_f^*} \int_{r^*=1}^{r_2^*} [T^*(r^*, t^*) - Y^*(r^*, t^*)]^2 \delta(r^* - r_m^*) \mathrm{d}r^* \mathrm{d}t^*$$

$$+\int_{t^*=0}^{t_f^*}\int_{r^*=1}^{r_2^*} r\cdot\lambda(r^*,t^*)\cdot\left[\frac{\partial^2 T^*}{\partial r^{*2}}+\left[\frac{1}{r^*}+\frac{\mathrm{d}k^*(r^*)/\mathrm{d}r^*}{k^*(r^*)}\right]\frac{\partial T^*}{\partial r^*}-\frac{1}{\alpha^*(r^*)}\frac{\partial T^*}{\partial t^*}\right]\mathrm{d}r^*\mathrm{d}t^* \tag{11}$$

The variation ΔJ is derived after $q^*(t^*)$ is perturbed by $\Delta q^*(t^*)$ and $T^*(r^*, t^*)$ is perturbed by $\Delta T^*(r^*, t^*)$ in Eq. (11). Subtracting from the resulting expression the original equation (11) and neglecting the second-order terms, we thus find:

$$\Delta J[q^*(t^*)] = \int_{t^*=0}^{t_f^*}\int_{r^*=1}^{r_2^*} 2[T^*(r^*,t^*)-Y^*(r^*,t^*)]\Delta T^*\cdot\delta(r^*-r_m^*)\mathrm{d}r^*\mathrm{d}t^*$$
$$+\int_{t^*=0}^{t_f^*}\int_{r^*=1}^{r_2^*} r\cdot\lambda(r^*,t^*)\cdot\left[\frac{\partial^2 \Delta T^*}{\partial r^{*2}}+\left[\frac{1}{r^*}+\frac{\mathrm{d}k^*(r^*)/\mathrm{d}r^*}{k^*(r^*)}\right]\frac{\partial \Delta T^*}{\partial r^*}-\frac{1}{\alpha^*(r^*)}\frac{\partial \Delta T^*}{\partial t^*}\right]\mathrm{d}r^*\mathrm{d}t^* \tag{12}$$

where $\delta(\cdot)$ is the Dirac function. We can integrate the second and third triple integral terms in Eq. (12) by parts, utilizing the initial and boundary conditions of the sensitivity problem. Then ΔJ is allowed to go to zero. The vanishing of the integrands containing ΔT^* leads to the following adjoint problem for the determination of $\lambda(r^*, t^*)$:

$$\frac{\partial^2\lambda}{\partial r^{*2}}+\left[\frac{1}{r^*}-\frac{\mathrm{d}k^*(r^*)/\mathrm{d}r^*}{k^*(r^*)}\right]\frac{\partial\lambda}{\partial r^*}-\frac{1}{r^*}\frac{\mathrm{d}}{\mathrm{d}r^*}\left[r^*\cdot\frac{\mathrm{d}k^*(r^*)/\mathrm{d}r^*}{k^*(r^*)}\right]\lambda$$
$$+\frac{1}{\alpha^*(r^*)}\frac{\partial\lambda}{\partial t^*}+\frac{2[T^*(r^*,t^*)-Y^*(r^*,t^*)]\Delta T^*\cdot\delta(r^*-r_m^*)}{r^*}=0 \tag{13}$$

$$k^*(r^*)\frac{\partial\lambda}{\partial r^*}=\frac{\mathrm{d}k^*(r^*)}{\mathrm{d}r^*}\lambda,\quad \text{at } r^*=r_1^* \tag{14}$$

$$k^*(r^*)\frac{\partial\lambda}{\partial r^*}+\left[Bis-\frac{\mathrm{d}k^*(r^*)}{\mathrm{d}r^*}\right]\lambda=0,\quad \text{at } r^*=r_2^* \tag{15}$$

$$\lambda=0,\quad \text{for } t^*=t_f^* \tag{16}$$

The adjoint problem is different from the standard initial value problem in that the final time condition at time $t^* = t_f^*$ is specified instead of the customary initial condition at time $t^* = 0$. However, this problem can be transformed to an initial value problem by the transformation of the time variable as $\tau^* = t_f^* - t^*$. Then the adjoint problem can be solved by the same method as the direct problem.

Finally the following integral term is left:

$$\Delta J=\int_{t^*=0}^{t_f^*} r^*\cdot\lambda(r_1^*,t^*)\cdot\Delta q^*(t^*)/k^*(r_1^*)\mathrm{d}t^* \tag{17}$$

From the definition used in Ref. [5], we have:

$$\Delta J=\int_{t^*=0}^{t_f^*} J'(t^*)\Delta q^*(t^*)\mathrm{d}t^* \tag{18}$$

where $J'(t^*)$ is the gradient of the functional $J(q)$. A comparison of Eqs. (6) and (7) leads to the following form:

$$J'(t^*) = r_1^* \cdot \lambda(r_1^*, t^*)/k^*(r_1^*) \tag{19}$$

Conjugate Gradient Method for Minimization

The following iteration process based on the conjugate gradient method is now used for the estimation of $q^*(t^*)$ by minimizing the above functional $J[q^*(t^*)]$

$$q^{*K+1}(t^*) = q^{*K}(t^*) - \beta^K p^K(t^*), \quad K = 0, 1, 2, \ldots \tag{20}$$

where β^K is the search step size in going from iteration K to iteration $K+1$, and $p^K(t^*)$ is the direction of descent (i.e., search direction) given by

$$p^K(t^*) = J'^K(t^*) + \gamma^K p^{K-1}(t^*) \tag{21}$$

which is conjugation of the gradient direction $J'^K(t^*)$ at iteration K and the direction of descent $p^{K-1}(t^*)$ at iteration $K-1$. The conjugate coefficient γ^K is determined from

$$\gamma^K = \frac{\int_{t^*=0}^{t_f^*} [J'^K(t^*)]^2 \mathrm{d}t^*}{\int_{t^*=0}^{t_f^*} [J'^{K-1}(t^*)]^2 \mathrm{d}t^*} \quad \text{with } \gamma^0 = 0 \tag{22}$$

The convergence of the above iterative procedure in minimizing the functional J is proved in Ref. [5]. To perform the iterations according to Eq. (20), we need to compute the step size β^K and the gradient of the functional $J'^K(t^*)$.

The functional $J[q^{*K+1}(t^*)]$ for iteration $K+1$ is obtained by rewriting Eq. (6) as:

$$J[q^{*K+1}(t^*)] = \int_{t^*=0}^{t_f^*} [T^*(q^{*K} - \beta^K p^K) - Y^*(r_m^*, t^*)]^2 \mathrm{d}t^* \tag{23}$$

where we replace q^{*K+1} by the expression given by Eq. (20). If temperature $T^*(q^{*K} - \beta^K p^K)$ is linearized by a Taylor expansion, Eq. (23) takes the form:

$$J[q^{*K+1}(t^*)] = \int_{t^*=0}^{t_f^*} [T^*(q^{*K}) - \beta^K \Delta T^*(p^K) - Y^*(r_m^*, t^*)]^2 \mathrm{d}t^* \tag{24}$$

where $T^*(q^{*K})$ is the solution of the direct problem at $r^* = r_m^*$ by using estimated $q^{*K}(t^*)$ for exact $q^*(t^*)$ at time t^*. The sensitivity function $\Delta T^*(p^K)$ are taken as the solution of Eqs. (7)–(10) at the measured position $r^* = r_m^*$ by letting $\Delta q^* = p^K$ [5]. The search step size β^K is determined by minimizing the functional given by Eq. (13) with respect to β^K. The following expression can be obtained:

$$\beta^K = \frac{\int_{t^*=0}^{t_f^*} \Delta T^*(p^K)[T^*(q^{*K}) - Y^*] \mathrm{d}t^*}{\int_{t^*=0}^{t_f^*} [\Delta T^*(p^K)]^2 \mathrm{d}t^*} \tag{25}$$

Stopping Criterion

If the problem contains no measurement errors, the traditional check condition specified as

$$J(q^{*K+1}) < \eta \tag{26}$$

where η is a small specified number, can be used as the stopping criterion. However, the observed temperature data contains measurement errors; as a result, the inverse solution will tend to approach the perturbed input data, and the solution will exhibit oscillatory behavior as the number of iteration is increased [17]. Computational experience has shown that it is advisable to use the discrepancy principle [15] for terminating the iteration process in the conjugate gradient method. Assuming $T^*(r_m^*, t^*) - Y^*(r_m^*, t^*) \cong \sigma$, the stopping criteria η by the discrepancy principle can be obtained from Eq. (6) as

$$\eta = \sigma^2 t_f^* \tag{27}$$

where σ is the standard deviation of the measurement error. Then the stopping criterion is given by Eq. (26) with η determined from Eq. (27).

Computational Procedure

The computational procedure for the solution of this inverse problem may be summarized as follows:

Suppose $q^{*K}(t^*)$ is available at iteration K.

Step 1 Solve the direct problem given by Eqs. (1)–(4) for $T^*(r^*, t^*)$.
Step 2 Examine the stopping criterion given by Eq. (26) with η given by Eq. (27). Continue if not satisfied.
Step 3 Solve the adjoint problem given by Eqs. (13)–(16) for $\lambda(r^*, t^*)$.
Step 4 Compute the gradient of the functional J' from Eq. (19).
Step 5 Compute the conjugate coefficient γ^K and direction of decent p^K from Eqs. (22) and (21), respectively.
Step 6 Set $\Delta q^*(t^*) = p^K(t^*)$ and solve the sensitivity problem given by Eqs. (7)–(10) for $\Delta T^*(r^*, t^*)$.
Step 7 Compute the search step size β^K from Eq. (25).
Step 8 Compute the new estimation for $q^{*K+1}(t^*)$ from Eq. (20) and return to Step 1.

Displacement and Thermal Stresses

To simplify the solving process, we introduce the following dimensionless variables:

$$E^* = E/E_0, \quad \omega^* = \omega/\omega_0, \quad u^* = u/\omega_0 T_0 r_1,$$
$$\sigma_r^* = \sigma_r/\omega_0 T_0 E_0, \quad \sigma_\theta^* = \sigma_\theta/\omega_0 T_0 E_0, \quad \sigma_z^* = \sigma_z/\omega_0 T_0 E_0 \tag{28}$$

where E_0 and ω_0 are reference values of elastic modulus and thermal expansion coefficient, respectively. Moreover, in this study, we also assume the elastic modulus

E, and thermal expansion coefficient ω change smoothly and continuously through the thickness of the FGM hollow circular cylinder.

Then, if the body forces are absent, the dimensionless equation of equilibrium for a symmetrical cylinder along the radial direction can be written as:

$$\frac{d\sigma_r^*(r^*, t^*)}{dr^*} + \frac{\sigma_r^*(r^*, t^*) - \sigma_\theta^*(r^*, t^*)}{r^*} = 0, \quad t > 0 \tag{29}$$

and the equations of equilibrium along the two other directions are satisfied identically.

The dimensionless mechanical boundary conditions are

$$\sigma_r^*(r^*, t^*) = 0, \quad \text{at } r^* = r_1^* \tag{30}$$

$$\sigma_r^*(r^*, t^*) = 0, \quad \text{at } r^* = r_2^* \tag{31}$$

which represent the traction-free conditions along the inner and outer surfaces, respectively.

The dimensionless stress and displacement relations are:

$$\sigma_r^*(r^*, t^*) = \frac{E^*}{(1+v)(1-2v)}\left[(1+v)\frac{du^*(r^*, t^*)}{dr^*} + v\frac{u^*(r^*, t^*)}{r^*}\right] - \frac{E^*\omega^*}{(1-2v)}T^*(r^*, t^*) \tag{32}$$

$$\sigma_\theta^*(r^*, t^*) = \frac{E^*}{(1+v)(1-2v)}\left[v\frac{du^*(r^*, t^*)}{dr^*} + (1+v)\frac{u^*(r^*, t^*)}{r^*}\right] - \frac{E^*\omega^*}{(1-2v)}T^*(r^*, t^*) \tag{33}$$

$$\sigma_z^*(r^*, t^*) = \frac{E^*}{(1+v)(1-2v)}\left[v\frac{du^*(r^*, t^*)}{dr^*} + v\frac{u^*(r^*, t^*)}{r^*}\right] - \frac{E^*\omega^*}{(1-2v)}T^*(r^*, t^*) \tag{34}$$

Generally, the Poisson's ratio v of FGM varies in a small range. For simplicity, we assume v to be a constant in this study.

By substituting stress-displacement relations (32) and (33) into equilibrium equation (29), the dimensionless field equation of displacement for the FGM hollow circular cylinder can be formulated as:

$$\frac{\partial^2 u^*}{\partial r^{*2}} + \left[\frac{1}{r^*} + \frac{dE^*(r^*)/dr^*}{E^*(r^*)}\right]\frac{\partial u^*}{\partial r^*} + \left[\frac{v}{1-v}\frac{dE^*(r^*)/dr^*}{E^*(r^*)} - \frac{1}{r^*}\right]\frac{u^*}{r^*} - \frac{1+v}{1-v}\frac{[\omega^*(r^*)\cdot E^*(r^*)]'}{E^*(r^*)}T^* - \frac{1+v}{1-v}\omega^*(r^*)\frac{\partial T^*}{\partial r^*} = 0 \tag{35}$$

Equation (35) can be solved by the method of central finite difference with the boundary conditions of Eqs. (30) and (31) once the temperature distributions $T^*(r^*, t^*)$ have been obtained by the inverse method.

RESULTS AND DISCUSSION

In the current paper, we consider a molybdenum/mullite functionally graded hollow circular cylinder. The inner and outer surfaces are pure mullite and composite of molybdenum/mullite, respectively. Both molybdenum and mullite vary continuously from the inner to outer surfaces of the cylinder. The values for k_0, α_0, E_0, ω_0, and v of the mullite taken from reference [14] are $5.9\,\mathrm{Wm^{-1}K^{-1}}$, $2.8 \times 10^{-6}\,\mathrm{m^2\,s^{-1}}$, $225\,\mathrm{GPa}$, $4.8 \times 10^{-6}\,\mathrm{K^{-1}}$, and 0.3, respectively. It is assumed that variations of the material properties through the thickness of the FGM hollow circular cylinder obey the following exponential laws [11]:

$$E^*(r^*) = \exp[m_1(r^* - r_1^*)] \tag{36}$$

$$\omega^*(r^*) = \exp[m_2(r^* - r_1^*)] \tag{37}$$

$$k^*(r^*) = \exp[m_3(r^* - r_1^*)] \tag{38}$$

$$\alpha^*(r^*) = \exp[m_4(r^* - r_1^*)] \tag{39}$$

where m_1, m_2, m_3, and m_4 are material constants, and they are $m_1 = 2.0, m_2 = 0.3, m_3 = 3.0$, and $m_4 = 2.0$, respectively, in the following numerical analysis. In addition, the values of r_1^*, r_2^*, and Bis are set as $r_1^* = 1.0, r_2^* = 2.0$, and $Bis = 2.0$, respectively. Moreover, a single thermocouple is assumed to be located at the inner surface ($r_m^* = r_1^*$). In terms of the time domain, the total dimensionless measurement time is chosen as $t_f^* = 1.0$ and measurement time step is taken to be 0.02.

The objective of this article is to validate the present approach when used in estimating the unknown time-dependent heat flux at the inner surface of a functionally graded hollow circular cylinder accurately with no prior information on the functional form of the unknown quantities, a procedure called function estimation. In order to illustrate the accuracy of the present inverse analysis, we consider the simulated exact value of $q^*(t^*)$ as

$$q^*(t^*) = 1 - \exp(-10t^*) \tag{40}$$

In the analysis, we do not have a real experimental setup to measure the temperature $Y^*(r_m^*, t^*)$ in Eq. (6). Instead, we assume a real heat flux, $q^*(t^*)$ of Eq. (26), and substitute the exact $q^*(t^*)$ into the direct problem of Eqs. (1)–(4) to calculate the temperatures at the location where the thermocouple is placed. The results are taken as the computed temperature $Y^*_{\mathrm{exact}}(r_m^*, t^*)$. Nevertheless, in reality, the temperature measurements always contain some degree of error, whose magnitude depends upon the particular measuring method employed. In order to consider the situation of measurement errors, a random error noise is added to the above computed temperature $Y^*_{\mathrm{exact}}(r_m^*, t^*)$ to obtain the measured temperature $Y^*(r_m^*, t^*)$. Hence, the measured temperature $Y^*(r_m^*, t^*)$ is expressed as

$$Y^*(r_m^*, t^*) = Y^*_{\mathrm{exact}}(r_m^*, t^*) + \varpi\sigma \tag{41}$$

where ϖ is a random variable within -2.576 to 2.576 for a 99% confidence bounds, and σ is the standard deviation of the measurement. The measured temperature $Y^*(r_m^*, t^*)$ generated in such way is the so-called simulated measurement temperature, and the temperature measurement is the so-called simulated temperature measurement.

The inverse solutions obtained from the numerical experiments with the initial guess values $q^{*0}(t^*) = 0.0$, and measurement errors $\sigma = 0.00, 0.01$, and 0.02, respectively, are shown in Figure 2. The iteration number K is equal to 15 and the temperature $Y^*(r_m^*, t^*)$ is measured at $r_m^* = 1.0$. These results confirm that the estimated results are in very good agreement with those of the exact values. For a temperature of unity and 99% confidence, the standard deviations $\sigma = 0.01$ and $\sigma = 0.02$ correspond to measurement error of 2.58% and 5.16%, respectively. The results in Figure 2 also demonstrate that, for the cases considered in this study, an increase in the measurement error does not cause obvious deterioration on the accuracy of the inverse solution. Meanwhile, to investigate the influence of measurement location upon the estimated results, Figure 3 illustrates the estimated unknown function $q^*(t^*)$, with temperature measurement taken at $r_m^* = 1.05$. Here, the initial guesses $q^{*0}(t^*) = 0.0$, iteration number $K = 15$, and measurement error $\sigma = 0.00, 0.01$, and 0.02, respectively. Satisfactory results are still returned, which has proved that different measurement locations pose no influence on the accuracy of the present inverse method.

Finally, Figures 4–7 demonstrate the prediction of temperature and thermal stresses in the FGM hollow circular cylinder along the radial direction for $t^* =$ 0.1, 0.4, and 0.8, respectively, which are obtained with the initial guesses $q^{*0}(t^*) =$ 0.0, temperature measurement taken at $r_m^* = 1.0$, iteration number $K = 15$, and measurement error of deviation $\sigma = 0.00$, 0.01, and 0.02, respectively. It can

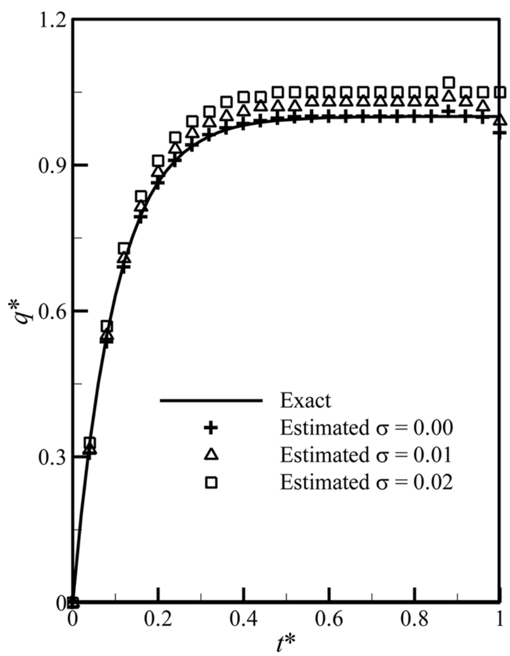

Figure 2 Estimated $q^*(t^*)$ at 15th iteration with initial guesses $q^{*0}(t^*) = 0.0$, $r_m^* = 1.0$, and $\sigma = 0.00$, 0.01, and 0.02, respectively.

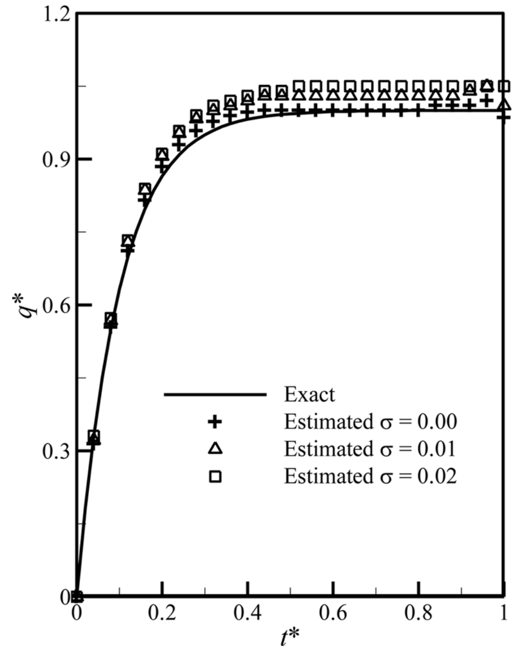

Figure 3 Estimated $q^*(t^*)$ at 15th iteration with initial guesses $q^{*0}(t^*) = 0.0$, $r_m^* = 1.05$, and $\sigma = 0.00$, 0.01, and 0.02, respectively.

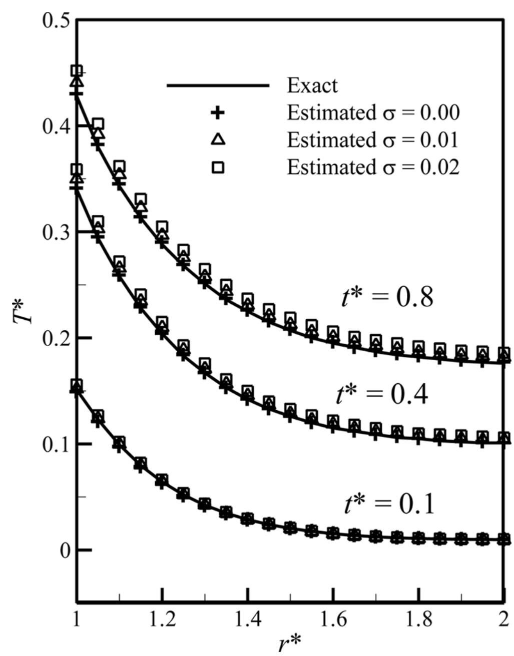

Figure 4 Estimated temperature distributions for various times at 15th iteration with initial guesses $q^{*0}(t^*) = 0.0$, $r_m^* = 1.0$, and $\sigma = 0.00$, 0.01, and 0.02, respectively.

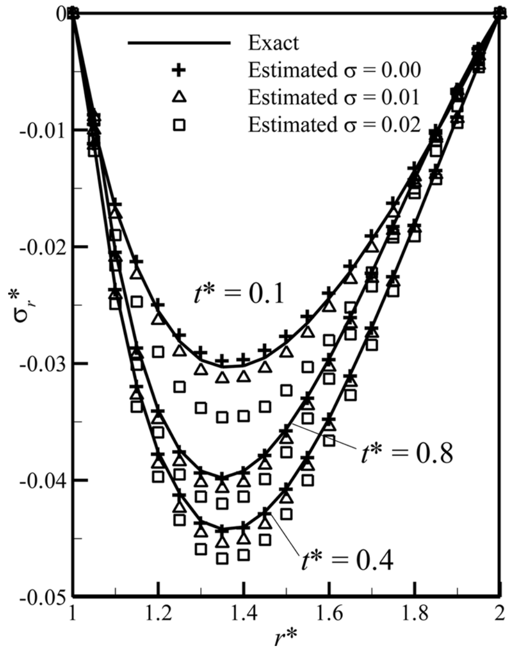

Figure 5 Estimated radial stress distributions for various times at 15th iteration with initial guesses $q^{*0}(t^*) = 0.0$, $r_m^* = 1.0$, and $\sigma = 0.00$, 0.01, and 0.02, respectively.

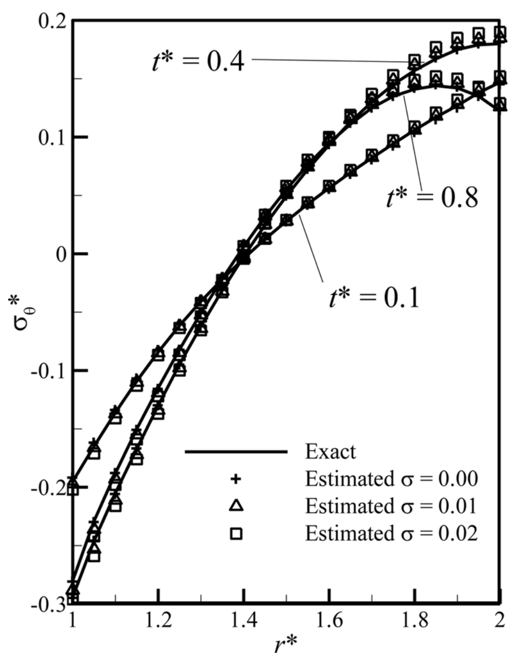

Figure 6 Estimated tangential stress distributions for various times at 15th iteration with initial guesses $q^{*0}(t^*) = 0.0$, $r_m^* = 1.0$, and $\sigma = 0.00$, 0.01, and 0.02, respectively.

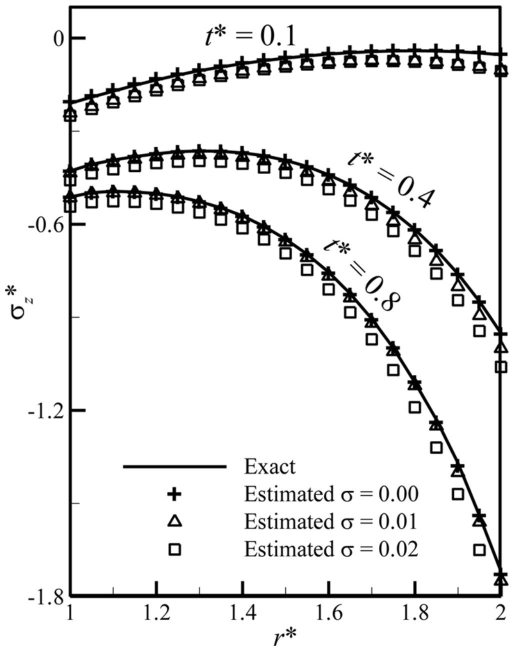

Figure 7 Estimated axial stress distributions for various times at 15th iteration with initial guesses $q^{*0}(t^*) = 0.0$, $r_m^* = 1.0$, and $\sigma = 0.00$, 0.01, and 0.02, respectively.

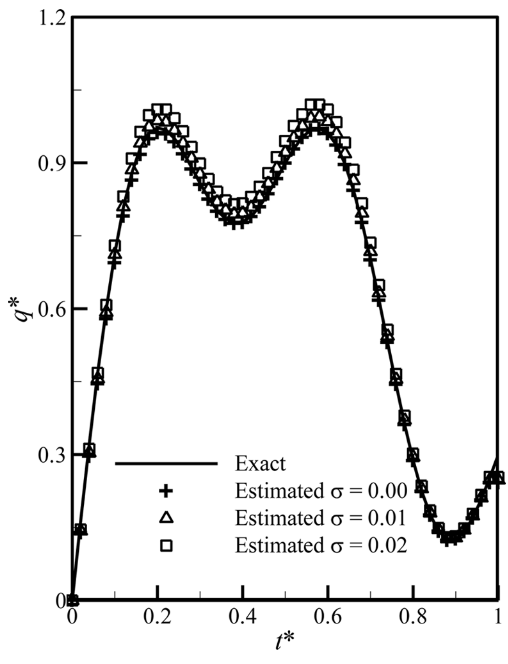

Figure 8 Estimated $q^*(t^*)$ at 15th iteration with initial guesses $q^{*0}(t^*) = 0.0$, $r_m^* = 1.0$, and $\sigma = 0.00$, 0.01, and 0.02, respectively.

be found that the predicted results for the temperature and thermal stresses distributions are in excellent agreement with those of the exact values for the case considered in this study.

To demonstrate the capability of the presented methodology in obtaining an accurate estimation no matter how complex the unknown function is, we consider another case of $q^*(t^*)$ with the following form:

$$q^*(t^*) = [0.3 \times \sin(2\pi t^*) + 0.25 \times \sin(4\pi t^*) + 3t^* \times (1.1 - t^*)] \tag{42}$$

Figure 8 shows the estimated results of $q^*(t^*)$, obtained with the initial guesses $q^{*0}(t^*) = 0.0$, temperature measurement taken at $r_m^* = 1.0$, iteration number $K = 15$, and measurement error of deviation $\sigma = 0.00, 0.01$, and 0.02, respectively. It can be found in Figure 8 that an excellent estimation still can be obtained with this complex unknown function.

CONCLUSION

An inverse algorithm based on the conjugate gradient method and the discrepancy principle was successfully applied for the solution of the inverse problem to determine the unknown time-dependent heat flux at the inner surface of a functionally graded hollow circular cylinder, while knowing the temperature history at some measurement locations. Subsequently, the temperature distributions and thermal stresses in the medium can be calculated as well. Numerical results confirm that the method proposed herein can accurately estimate the time-dependent heat flux, temperature distributions, and thermal stresses for the problem even involving the inevitable measurement errors. The proposed inverse algorithm does not require prior information for the functional form of the unknown quantities to perform the inverse calculation, and excellent estimated values can be obtained for the considered problem.

NOMENCLATURE

E	elastic modulus (GPa)
h	convection heat transfer coefficient ($Wm^{-2}K^{-1}$)
J	functional
J'	gradient of functional
k	thermal conductivity ($Wm^{-1}K^{-1}$)
p	direction of descent
q	heat flux at the inner surface (W/m^2)
r	radial coordinate (m)
r_1	inner radius of the cylinder (m)
r_2	outer radius of the cylinder (m)
T	temperature (K)
T_0	reference temperature (K)
T_∞	outer surrounding temperature (K)
t	time coordinate (s)
u	displacement radial component (m)

Greek Symbols

Δ	small variation quality
α	thermal diffusivity ($m^2\,s^{-1}$)
β	step size
γ	conjugate coefficient
η	very small value
λ	variable used in the adjoint problem
σ	standard deviation
σ_r	stress radial component (MPa)
σ_z	stress axial component (MPa)
σ_θ	stress tangential component (MPa)
τ	transformed time coordinate
ω	thermal expansion coefficient (1/K)
ϖ	random variable

Superscripts/Subscripts

K	iterative number
$*$	dimensionless quantity

REFERENCES

1. H. L. Lee and Y. C. Yang, Function Estimation in Predicting Time-Dependent Heat Flux of an Annular Fin, *J. Therm. Stresses*, vol. 26, pp. 799–813, 2003.
2. C. R. Su and C. K. Chen, Geometry Estimation of the Furnace Inner Wall by an Inverse Approach, *Int. J. Heat Mass Trans.*, vol. 50, pp. 3767–3773, 2007.
3. C. Y. Yang, Direct and Inverse Solutions of the Two-Dimensional Hyperbolic Heat Conduction Problems, *Appl. Math. Model.*, vol. 33, pp. 2907–2918, 2009.
4. W. L. Chen and Y. C. Yang, Inverse Estimation for the Unknown Fouling-Layer Profiles with Arbitrary Geometries on the Inner Wall of a Forced-Convection Duct, *Int. J. Thermal Sci.*, vol. 49, pp. 86–98, 2010.
5. O. M. Alifanov, *Inverse Heat Transfer Problem*, Springer-Verlag, New York, 1994.
6. W. L. Chen and Y. C. Yang, Estimation of the Transient Heat Transfer Rate at the Boundary of an Electronic Chip Packaging, *Numer. Heat Trans. A*, vol. 54, pp. 945–961, 2008.
7. C. H. Huang, L. Y. Chen, and S. Kim, An Inverse Geometry Design Problem in Optimizing the Shape of Gas Channel for Proton Exchange Membrane Fuel Cell, *J. Power Sources*, vol. 187, pp. 136–147, 2009.
8. W. L. Chen and Y. C. Yang, Simultaneous Estimation of Heat-Transfer Rate and Coolant Fluid Velocity in a Transpiration Cooling Proces, *Int. J. Thermal Sci.*, vol. 49, pp. 1407–1416, 2010.
9. C. Le Niliot and F. Lefevre, Multiple Transient Point Heat Source Identification in Heat Diffusion: Application to Numerical Two- and Three-Dimensional Problem, *Numer. Heat Trans. B*, vol. 39, pp. 277–301, 2001.
10. M. Raudensky, K. A. Woodbury, and J. Kral, Genetic Algorithm in Solution of Inverse Heat Conduction Problems, *Numer. Heat Trans. B*, vol. 28, pp. 293–306, 1995.
11. Z. S. Shao, T. J. Wang, and K. K. Ang, Transient Thermo-Mechanical Analysis of Functionally Graded Hollow Circular Cylinders, *J. Therm. Stresses*, vol. 30, pp. 81–104, 2007.

12. Y. Ootao and Y. Tanigawa, Transient Thermoelastic Analysis for a Laminated Composite Strip with an Interlayer of Functionally Graded Material, *J. Therm. Stresses*, vol. 32, pp. 1181–1197, 2007.
13. Y. Ootao and Y. Tanigawa, Transient Thermoelastic Problem of a Functionally Graded Hollow Cylinder due to Asymmetrical Surface Heating, *J. Therm. Stresses*, vol. 32, pp. 1217–1234, 2009.
14. M. R. Golbahar Haghighi, M. Eghtesad, P. Malekzadeh, and D. S. Necsulescu, Two-Dimensional Inverse Heat Transfer Analysis of Functionally Graded Materials in Estimating Time-Dependent Surface Heat Flux, *Numer. Heat Trans. B*, vol. 54, pp. 744–762, 2008.
15. O. M. Alifanov and E. A. Artyukhin, Regularized Numerical Solution of Nonlinear Inverse Heat-Conduction Problem, *J. Eng. Phys.*, vol. 29, pp. 934–938, 1975.
16. Y. C. Yang, H. L. Lee, J. C. Hsu, and S. S. Chu, Thermal Stresses in Multilayer Gun Barrel with Interlayer Thermal Contact Resistance, *J. Therm. Stresses*, vol. 31, pp. 624–637, 2008.
17. O. M. Alifanov, Application of the Regularization Principle to the Formulation of Approximate Solution of Inverse Heat Conduction Problem, *J. Eng. Phys.*, vol. 23, pp. 1566–1571, 1972.